Theoretical investigation on the mechanism and kinetics of the ring-opening polymerization of ε-caprolactone initiated by tin(II) alkoxides

ARTICLE *in* JOURNAL OF MOLECULAR MODELING · OCTOBER 2013

Impact Factor: 1.74 · DOI: 10.1007/s00894-013-2026-2 · Source: PubMed

5 AUTHORS, INCLUDING:

Chanchai Sattayanon
Chiang Mai University
4 PUBLICATIONS **7** CITATIONS
SEE PROFILE

Nawee Kungwan
Chiang Mai University
54 PUBLICATIONS **217** CITATIONS
SEE PROFILE

Puttinan Meepowpan
Chiang Mai University
39 PUBLICATIONS **195** CITATIONS
SEE PROFILE

Siriporn Jungsuttiwong
Ubon Ratchathani University
81 PUBLICATIONS **879** CITATIONS
SEE PROFILE

J Mol Model (2013) 19:5377–5385
DOI 10.1007/s00894-013-2026-2

ORIGINAL PAPER

Theoretical investigation on the mechanism and kinetics of the ring-opening polymerization of ε-caprolactone initiated by tin(II) alkoxides

Chanchai Sattayanon · Nawee Kungwan · Winita Punyodom · Puttinan Meepowpan · Siriporn Jungsuttiwong

Received: 27 December 2012 / Accepted: 30 September 2013 / Published online: 31 October 2013

Abstract A theoretical investigation of the ring-opening polymerization (ROP) mechanism of ε-caprolactone (CL) with tin(II) alkoxide, $Sn(OR)_2$ initiators (R=*n*-C_4H_9, *i*-C_4H_9, *t*-C_4H_9, *n*-C_6H_{13}, *n*-C_8H_{17}) was studied. The density functional theory at B3LYP level was used to perform the modeled reactions. A coordination-insertion mechanism was found to occur via two transition states. Starting with a coordination of CL onto tin center led to a nucleophilic addition of the carbonyl group of CL, followed by the exchange of alkoxide ligand. The CL ring opening was completed through classical acyl-oxygen bond cleavage. The reaction barrier heights of ε-caprolactone with different initiators were calculated using potential energy profiles. The reaction of ε-caprolactone with $Sn(OR)_2$ having R=*n*-C_4H_9 has the least value of barrier height compared to other reactions. The rate constants for each reaction were calculated using the transition state theory with TheRATE program. The rate constants are in good agreement with available experimental data.

Keywords Coordination-insertion mechanism · Density functional theory · ε-caprolactone · Ring-opening polymerization · Tin(II) alkoxides · Transition state theory

Introduction

Poly(ε-caprolactone) (PCL), synthetic biodegradable and biocompatible polymer, has been extensively studied due to its medical and environmental applications [1]. The biomedical uses are in areas of controlled release drug delivery systems [2–5] and 3D scaffolds for use in tissue engineering [6]. The environmental friendly uses are in the area of disposable packaging [7]. The most widely used technique for synthesizing this polymer and its related aliphatic polyesters is the ring opening polymerization (ROP) [8]. The ROP of cyclic esters [9] can be achieved by using cationic, anionic, activated monomer, enzymatic, and organocatalytic methods [10]. A large number of experimental studies have been carried out with different catalyst or initiator of metal alkoxides in which metals can be alkali [11, 12], transition [13–16], and lanthanide [17, 18]. Metal alkoxides are the most widely used types of ROP initiator and their ring opening mechanism is coordination-insertion of monomer into the metal-oxygen bond of initiator. To date, the most widely use metal alkoxide both in academia and industry is $Sn(Oct)_2$ [9, 19–24]. Many research groups have used $Sn(Oct)_2$ with alcohol to study the ROP of different kinds of monomers. It is widely accepted that the $Sn(Oct)_2$ initiator and ROH co-initiator react together in situ to form the corresponding tin(II) monoalkoxide, [Sn(Oct)(OR)], and/or dialkoxide, [$Sn(OR)_2$] which are the "true initiator". However, the true initiator has to be formed prior to ROP initiation and

Electronic supplementary material The online version of this article (doi:10.1007/s00894-013-2026-2) contains supplementary material, which is available to authorized users.

C. Sattayanon · N. Kungwan · W. Punyodom · P. Meepowpan
Center of Excellence for Innovation in Chemistry, Department of Chemistry, Faculty of Science, Chiang Mai University, Chiang Mai, Thailand 50200

N. Kungwan (✉) · W. Punyodom · P. Meepowpan
Biomedical Polymers Technology Unit, Department of Chemistry, Faculty of Science, Chiang Mai University, Chiang Mai, Thailand 50200
e-mail: naweekung@gmail.com

S. Jungsuttiwong
Center for Organic Electronic and Alternative Energy, Department of Chemistry and Center of Excellence for Innovation in Chemistry, Faculty of Science, Ubon Ratchathani University, Ubon Ratchathani, Thailand 34190

propagation which leads to an inevitable long induction time. Furthermore, the molecular weight of desired polymers cannot be precisely controlled using $Sn(Oct)_2$ because the true initiator is not formed directly in the first state. To reduce this induction time and also obtain polymers with highly controlled molecular weight, a novel tin(II) alkoxide initiator was introduced [25, 26] with more effective molecular weight control and less reduction time. The ROP mechanism of cyclic esters with metal alkoxide initiators has been proposed to follow the states illustrated in our adapted Scheme 1 [9, 27, 28]. In the adapted schematic diagram, Sn atom is used to represent any metal in the metal alkoxide initiators and ε-caprolactone represents any cyclic ester monomer. The detail information on the ROP mechanism shown in Scheme 1 is described in the following five steps:

1. *Complex*: The initial step involves the weak complexation of CL and tin(II) alkoxide. The weak **complex** can be formed by a coordination interaction between CL and tin(II) alkoxide initiator. An electrophilic attack by carbonyl group of CL onto the nucleophilic Sn atom of tin(II) alkoxide is attained.
2. *TS1*: The second step is the first transition state (**TS1**) formation. This four-membered ring transition state is formed by introducing the new bond between Sn and oxygen atom on the carbonyl group of CL.
3. *Intermediate*: The third step is the stable intermediate formation. This intermediate is formed by rotating the alkoxyl (−OR) group away from the Sn atom and the weak interaction between Sn and oxygen atom is attained.
4. *TS2*: The forth step involves the formation of second transition state (**TS2**). This transition state can be achieved by making a covalent bond of Sn atom to the oxygen atom adjacent to the carbonyl group. The high constraint four-membered ring transition is readily open to the CL forming the **product**.
5. *Product*: The final step is the **product** formation. This **product** is the consequence of ring-opening of **TS2** species. The second monomer of CL can be added into this **product** and the propagation of next ring-opening polymerization is continued.

The detailed information on the molecular level of ROP of CL with true initiator can be revealed only by means of theoretical study. Some theoretical investigations using density function theory (DFT) on the ROP of CL with various initiators have been employed [11, 29–33]. In this present work the ROP polymerization mechanism of ε-CL with tin(II) alkoxide initiators will be investigated by quantum chemical calculations. Geometries, energies, and vibrational frequencies of all stationary points (reactant, transition state, intermediate, and **product**) along the reaction profiles shown in Scheme 1 will be explored using DFT at B3LYP method with mixed basis set. The calculated results will be analyzed to give the energy profile and to compare the effect of different R groups on the initiators. Furthermore, information derived from energy profiles will be used to calculate the rate

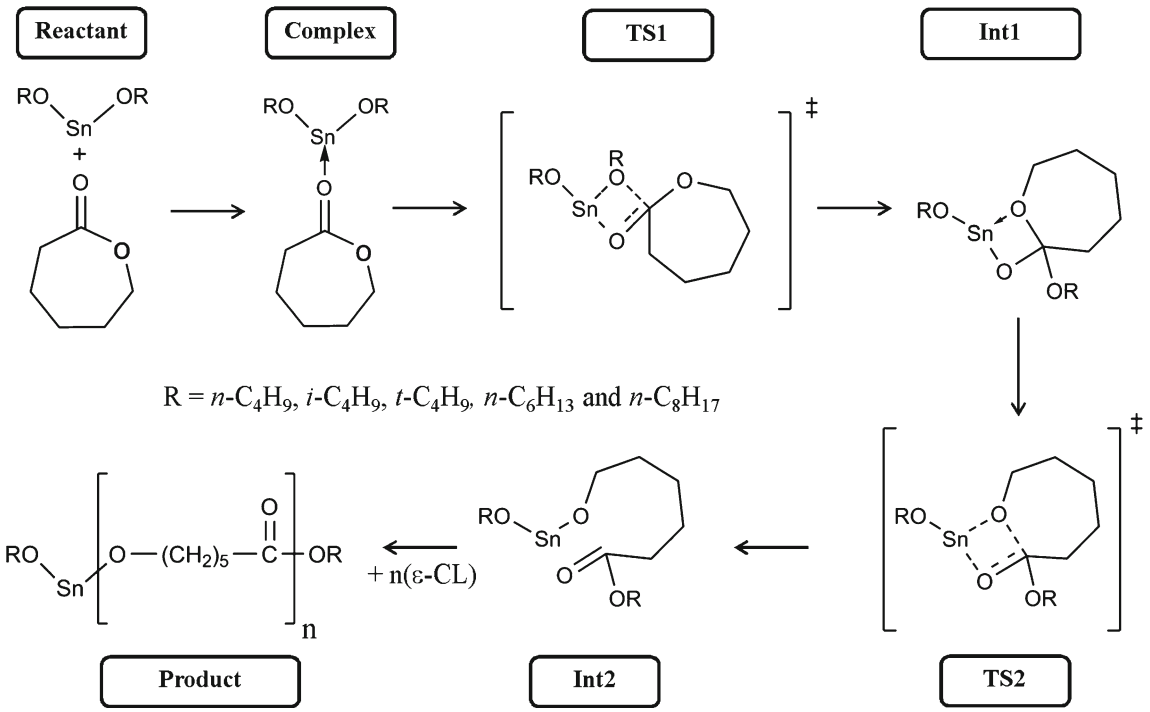

Scheme 1 The mechanism for ring-opening polymerization of ε-caprolactone initiated by tin(II) alkoxides

constants of different initiators using transition state theory (TST).

Computational details

Quantum chemical calculation was used to investigate the ROP mechanism of CL initiated by tin(II) alkoxides, $Sn(OR)_2$ when R=*n*-C_4H_9(*n*-But), *i*-C_4H_9(*i*-But), *t*-C_4H_9(*t*-But), *n*-C_6H_{13}(*n*-Hex) and *n*-C_8H_{17}(*n*-Oct). Geometries, energies, and vibrational frequencies of all stationary points (reactant, **complex**, transition state, intermediate and **product**) along with reaction profiles were computed using the hybrid density functional theory (DFT) at B3LYP level [34]. For metal atom, a doublet-ζ-valence quality basis set LANL2DZ was assigned for Sn atom. A relativistic electron core potential (ECP) developed by Hay and Wadt replaced the Sn core electron [35, 36]. For non-metal atoms, a valence triple zeta with polarization function (VTZ2P) at cc-pVTZ was assigned for C, H, and O atoms. This popular and computationally cost effective method predicted reliable geometries and energies as reported in previous studies [11, 30, 37]. The characters of intermediates and transition states were confirmed by performing frequency calculations [11, 38]. Furthermore, the connection between the reactive reactants (intermediate) and products was checked with the assistance of the intrinsic reaction coordinate (IRC) [39]. The IRC procedure was carried out using the step size of 20 and maxpoint of 10 both forward and reverse directions which means that reaction coordinate was calculated every 0.2 $amu^{1/2}$ bohr. The reaction barrier heights of all reactions were corrected by including the zero-point energy corrections [40]. All calculations were performed with the Gaussian03 software package [41].

The information obtained from quantum chemical calculations was employed to determine the thermal rate constants of the reactions. These thermal rate constants in temperature range of 100–120 °C were calculated using the conventional TST method [42] by University of Utah's web-based kinetics module within the Computational Science and Engineering Online suite (CSEOnline) [43]. Finally, the calculated rate constants will be compared with the available experimental data.

Results and discussion

The tin(II) butoxide assisted ROP coordination-insertion mechanism for monomer of CL was investigated by DFT(B3LYP) with mix basis set method. The corresponding DFT based optimized structures and energies of each step following Scheme 1 are depicted in Fig. 1 which is the ROP reaction of CL with $Sn(n\text{-OBut})_2$. This ROP diagram is used to represent the ROP mechanism of CL with Sn(II) alkoxides.

The ROP mechanism

The exo-carbonyl group of CL coordinates the Sn metal (**complex**) in the *cis* position with O^1, resulting in a Sn-O^2 distance of 2.61 Å. The energy of **complex** formation is −7.53 kcal mol^{-1}. The transformation of **complex** into **TS1** involves addition of the Sn-O^3 onto the C^1-O^2 double bond and a corresponding rotation of the O^1-C^1-O^2 plane 90° forming a planar four-membered ring (**TS1**) having sp^2-sp^3 hybridized C^1 which is located above that O^2-C^1-O^1 plane. This process lengthens the Sn-O^3 and shortens the Sn-O^2 (Fig. 1). It requires moderate energy (14.58 kcal mol^{-1}) and the supported DFT with only one negative imaginary frequency of −217 cm^{-1} is obtained. The correspondent vibrational mode to this imaginary frequency is shown in Fig. S1 of the Supplementary data. Furthermore, the IRC result confirms the connection between **complex** and **Int1** as shown in Fig. S2 of the Supplementary data. The nature bond orbital (NBO) charges along the reaction pathway on Sn and C^1 slightly decrease and on O^1 also decrease but those on O^2 and O^3 increase (Fig. 2). The slight change of natural bond orbital (electronic density) from the Lewis base of Sn was observed due to compensation from O^2 and O^3 to Sn of **Complex** and **TS1**.

The conversion of **TS1** to intermediate 1 (**Int1**) involves rotation of CL ring around the C^1-O^2 bond resulting in a decrease and an increase in the Sn-O^3 and Sn-O^1 distances, respectively (Fig. 1). The Sn-O^1 distance is about 3.41 Å which is not a bond between two atoms but only an attractive force between them (a normal bond distance of Sn-O is about 2.00 to 2.20 Å). The **Int1** energy is 9.2 kcal mol^{-1} above the **complex**. The optimized transition state 2, **TS2**, shows a four-membered ring with nearly equal Sn-O^1 and Sn-O^2 distances and a sp^3 hybridized C^1 atom with C^1-O^1, C^1-O^2 and C^1-O^3 bond lengths between 1.28 and 1.86 Å. This step is completely attained when the bond of Sn-O^1 is created. The **TS2** structure is confirmed by an imaginary frequency of −215 cm^{-1} (its correspondent vibrational mode with displacement vectors is shown in Fig. S3 of the Supplementary data) and IRC calculation indicates that a saddle point along the reaction pathway (between **Int1** and **Int2**) exists (see S4 in Supplementary data as an example of IRC results). This **TS2** eventually ruptures to intermediate 2 (**Int2**) and then forms **product** with increasing bond length of C^1-O^1. The information of the lowest frequencies in all species (**complex**, **TS1**, **Int1**, **TS2**, **Int2**, and **product**) is listed in Table S1 of the Supplementary data. Our DFT based calculation gave two transition state formation steps with the **TS1** being the rate-determining step. Our calculated results based on proposed mechanism in Scheme 1 of tin(II) butoxide with CL is found to be similar to the proposed ROP mechanism of $SnMe_3OMe$ with 1,5-dioxepan-2-one (DXO) reported by von Schenck and co-workers [11].

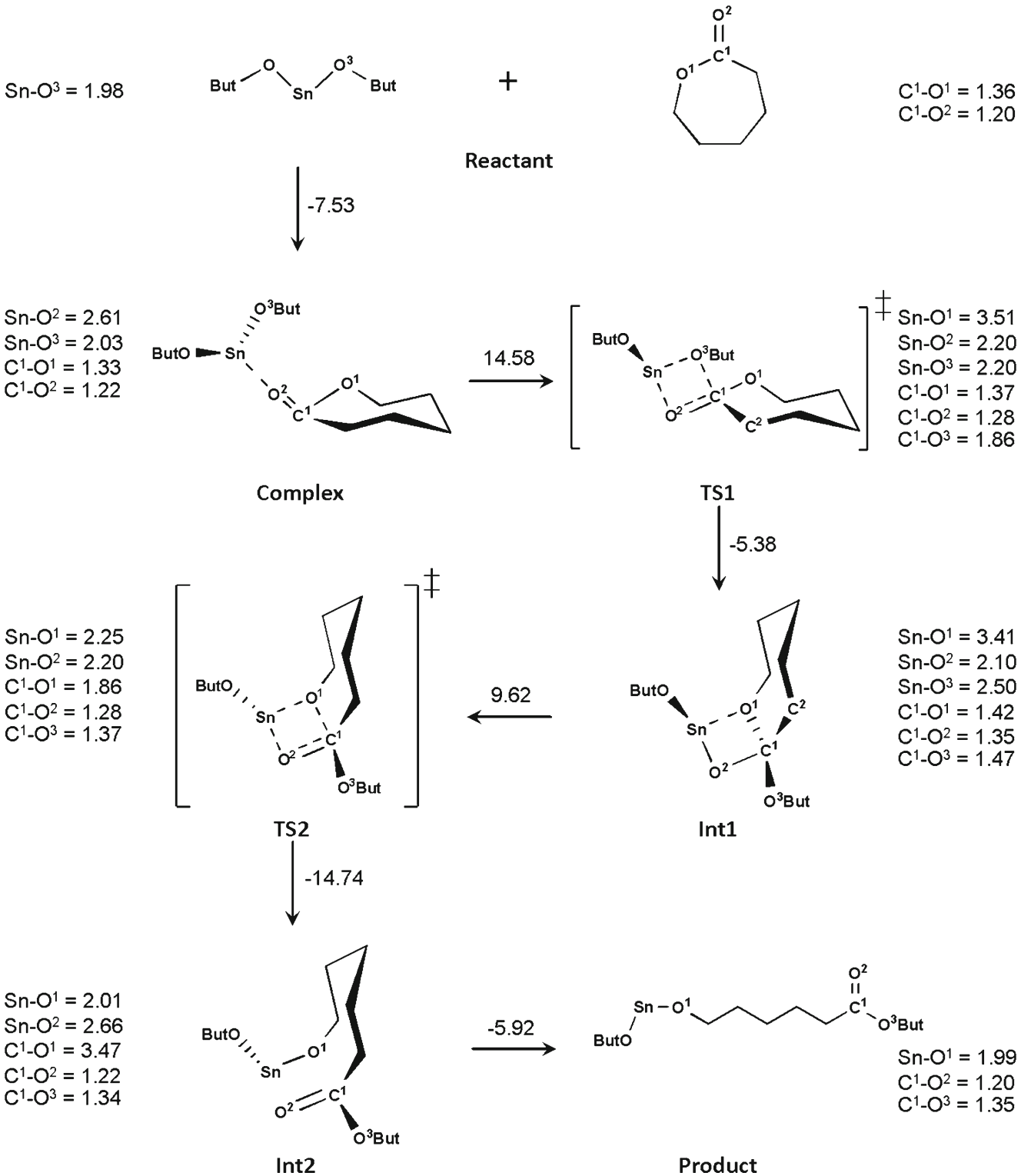

Fig. 1 ROP mechanism of CL initiated with Sn(*n*-OBut)$_2$. Bond lengths are in Å and the relative total energies (electronic energy + ZPE) are in kcal mol^{-1}

This may be due to the similarity of coordinate stability for Sn both in tetravalent and divalent forms. Moreover, the relative enthalpies of **product** compared to that of reactant of all initiators were found to be negative indicating that the overall ring opening polymerization reactions in all initiators is exothermic. The thermodynamic

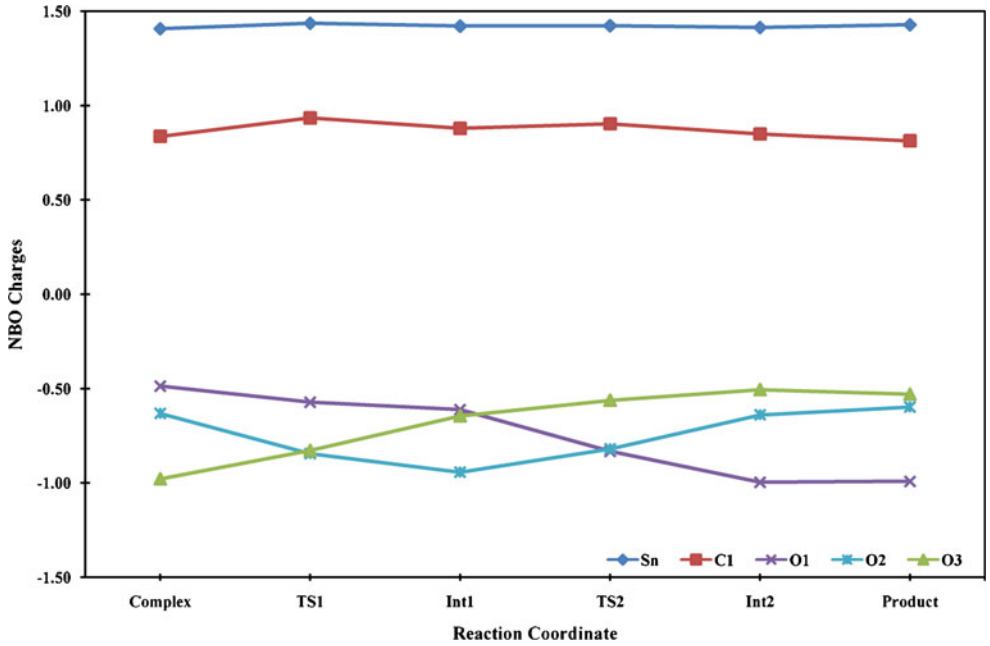

Fig. 2 Natural bond orbital charges of several atoms involved in the reaction intermediates in the polymerization of CL initiated by $Sn(OR)_2$ having R *n*-But

data of all species along the reaction path are listed in Table S3 of the Supplementary data.

Generally, ROP mechanisms of CL with other tin(II) alkoxides ($Sn(OR)_2$) namely: $Sn(n\text{-OHex})_2$, $Sn(n\text{-OOct})_2$, $Sn(i\text{-OBut})_2$, and $Sn(t\text{-OBut})_2$ are shown in S5–S8 of Supplementary data which are similar to that of CL with $Sn(n\text{-OBut})_2$. Two transition state steps formation (**TS1**, **TS2**) with four-membered ring of CL with initiators prior to ring-opening is found in all initiators. However, the relative energy changes as a function of reaction coordinate are quite different in some initiators, especially with bulky groups. So the effects of side chain and bulky group are given below.

Comparison of different initiators

Like in the case of CL with $Sn(n\text{-OBut})_2$, the DFT results of **complex** for CL with $Sn(n\text{-OHex})_2$ and $Sn(n\text{-OOct})_2$ give the identical $Sn\text{-}O^2$ distance of 2.61 Å implying that longer chain does not affect the stability of **complex** formation. The stability of different R groups depends on the bond distance of $Sn\text{-}O^3$ in reactant (initiator) and **complex**. The $Sn\text{-}O^3$ bonds of *t*-But and *i*-But are found to be shorter (1.97 Å) than that of other initiator (2.61 Å). The shorter the $Sn\text{-}O^3$ bond, the more stable the **complex** becomes which results in more energy required to break this bond. In addition for **complex**, the $Sn\text{-}O^3$ bond in *t*-But is found to be shortest (2.00 Å) compared to that of other initiators (2.03 Å). All important Sn-O bonds along the reaction path for all initiators are listed in Table S2 of the Supplementary data. Moreover, the NBO charge values of important atoms along the reaction path and the plots of NBO charges for all initiators were listed in Table S3 and plotted in Fig. S9–S12 of the Supplementary data.

The **complex** stability is found in the following order of R group: *t*-But > *n*-But > *n*-Hex > *i*-But > *n*-Oct (see Table 1). The formation of **TS1** for all four initiators requires moderate energy with the energy ranked as *t*-But > *i*-But = *n*-Oct > *n*-Hex > *n*-But which is in the order of energy somewhat difference from **complex** stability. This order of energy requirement may be explained by the stability of **TS1** by steric effect influence from the R group. The more bulky the R group, the more energy is required for **TS1** to be formed. Note that *i*-But and *n*-Oct have the same steric effect even though number of carbon atom on both are not the same. The confirmation of **TS1** formation with all initiators is confirmed with only one imaginary frequency and IRC calculation.

The conversion of **TS1** to intermediate for all four initiators proceeds similarly to the CL and $Sn(n\text{-OBut})_2$. The rotation of $C^1\text{-}O^2$ bond causes the $Sn\text{-}O^3$ and $Sn\text{-}O^1$ distances to decrease and increase respectively. The energy required for **TS2** to be formed is about 9.62 kcal mol^{-1} which is not as much as required for **TS1** (values can be obtained by subtracting the energy of **TS2** with energy of **Int** in Table 1 for **TS2** energy required and the energy of **TS1** with **complex** for **TS1** energy required). The existences of **TS2** for all four initiators are confirmed by frequency calculation with one imaginary number and IRC. Like in the case of tin(II) *n*-butoxide, **TS2** of these four initiators with driving force eventually ruptures to **Int2** prior to forming the **product**. The next cycle of a new monomer of CL will form **complex** and the propagation will be repeated to form a longer chain of polymer.

Table 1 and Fig. 3 summarize the energy changes of reactions of CL initiated by different $Sn(OR)_2$ initiators where R=*n*-But, *i*-But, *t*-But, *n*-Hex and *n*-Oct as a function of reaction progress. With similar geometries, **complex** (as

Table 1 The relative energies comparison in each initiator

Reaction coordination	Relative energy (kcal mol^{-1})				
	n-But	*n*-Hex	*n*-Oct	*i*-But	*t*-But
Reactant	0.00	0.00	0.00	0.00	0.00
Complex	−7.53	−7.48	−6.46	−6.91	−10.55
TS1	7.05	7.13	8.13	8.13	9.49
Int 1	1.67	1.77	2.73	3.88	6.19
TS2	11.29	11.38	12.43	12.82	15.37
Int 2	−3.45	−3.45	−2.41	−4.33	1.28
Product	−9.37	−9.42	−8.30	−8.13	−9.81

shown in S2–S5 in Supplementary data) can be regarded as being equivalent to **product**. Thus, the above DFT based mechanism may be applicable to both initiation and propagation. There are two main effects on the initiators to be discussed in more detail. First, the effect of long chain on R group in $Sn(OR)_2$ initiator starting from C_4(*n*-But) to C_6 (*n*-Hex) and C_8 (*n*-Oct) shows a slight energy change on the relative **TS1** energy. For *n*-But, *n*-Hex, and *n*-Oct the required energies are 7.05, 7.13 and 8.13 kcal mol^{-1}, respectively. The longer chain on R group slightly destabilizes the **TS1** formation stability. Therefore the shorter R group is more favorable to make the rate of reaction go faster within the same condition as **TS1** is the rate-determining step for ROP.

The calculated rate constants of each initiator and also some available experiment data are discussed in the next section. The initiators with R group greater than C_4 was considered in our study due to the solubility of initiators based on our experiment study. Second, the effect of branching group on butyl group in $Sn(OR)_2$ initiator from C_4(*n*-But) to *iso*-C_4 (*i*-But) and *tert*-C_4 (*t*-But) reveals significant change on energy of **TS1** formation. Obviously, the more steric hindrance of branching C_4, the less stable the **TS1** observed. The overall reaction of all initiators is found to be exothermic compared with reactants.

The thermal rate constants in the range of 100–120 °C were calculated using information from the quantum calculation with TST implemented in TheRATE program [25]. The calculated and experimental results are shown in Table 2 and plotted in Fig. 4. Both available experiment data and theoretical results correspond with TST in which the higher the temperature, the faster the rate constants becomes. Especially at 120 °C, the rate constants show the highest value.

The comparisons of rate constants between the experiment (▲) and the calculation (●) results were discussed. From the comparison, we found that rate constant results show an interesting value. For experimental results, the rate constants of Sn(*n*-OBut)$_2$, Sn(*n*-OHex)$_2$, Sn(*n*-OOct)$_2$, Sn(*i*-OBut)$_2$ and Sn(*t*-OBut)$_2$ are 118.70, 95.40, 20.10, 31.65 and 9.90 L mol^{-1} min^{-1}, respectively. Meanwhile, the rate

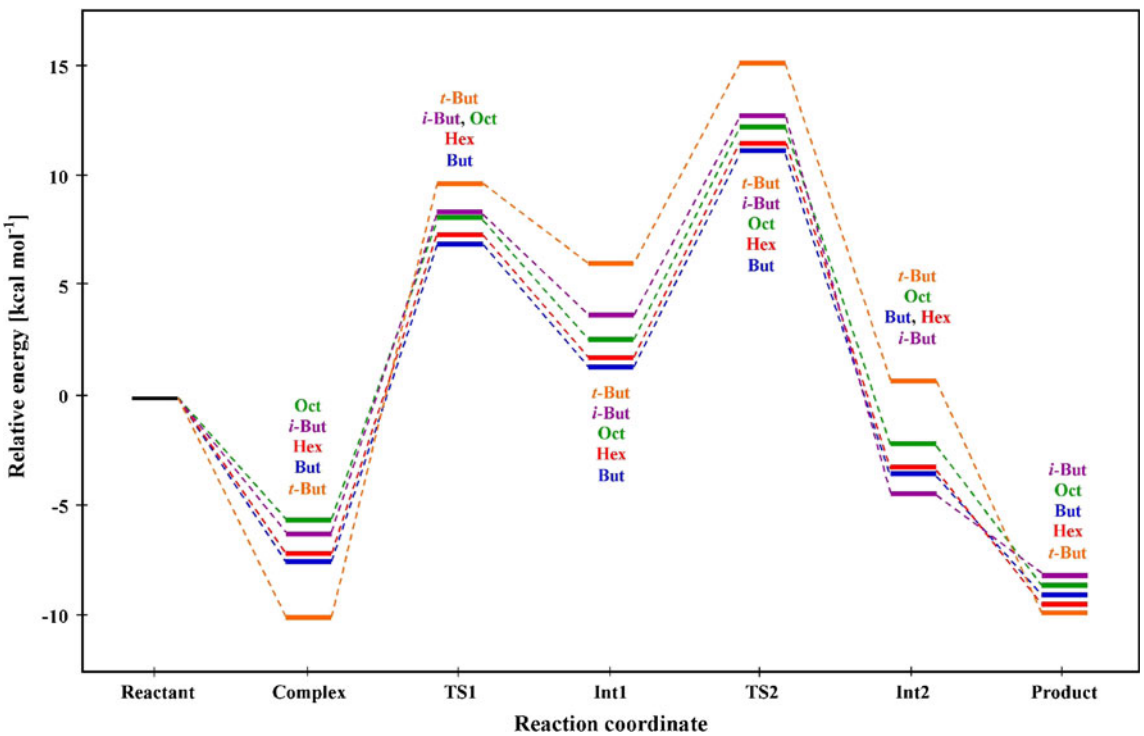

Fig. 3 Energy changes as a function of reaction progress for monomer addition for the ROP of CL with different $Sn(OR)_2$ initiators as R=*n*-But(blue), *i*-But(purple), *t*-But(orange), *n*-Hex(red), and *n*-Oct(green)

Table 2 The theoretical and experimental rate coefficient of all initiators

$Sn(OR)_2$	Temperature(°C)	Rate coefficient (L mol^{-1} min^{-1})	
		Experiment[a]	Theory[b]
n-But	100	55.80	33.57
	110	111.70	45.01
	120	118.70	59.56
n-Hex	100	34.30	20.12
	110	62.70	27.01
	120	95.40	35.81
n-Oct	100	13.10	9.11
	110	16.30	12.67
	120	20.10	17.37
i-But	100	-	14.09
	110	-	19.67
	120	31.65[c]	27.05
t-But	100	–	1.56
	110	–	2.29
	120	9.90[c]	3.31

[a] Calculated by dilatometry's measurement of Winita's group [25]

[b] Calculated by TheRATE program of University of Utah [43]

[c] These values were calculated by relative number

constants of all initiators in calculation results are 59.56, 35.81, 17.37, 27.05, and 3.31 L mol^{-1} min^{-1}, respectively. The calculated value is in good agreement within a factor of two compared with experimental data. Especially, tin(II) *n*-butoxide shows the highest rate constants compared with other initiators. It is indicated that tin(II) *n*-butoxide gives the highest reaction rate constant among the other initiators. These rate constant results are also related to the energy profile of tin(II) *n*-butoxide (Fig. 3) that is the lowest relative energy of rate-determining step (**TS1**) compared to the other initiators.

From the discussion above, we found that rate constant results are different due to two main factors. First, the effect of side chains, $Sn(n\text{-OBut})_2$, $Sn(n\text{-OHex})_2$, $Sn(n\text{-OOct})_2$, shows that the longer the chains, the more steric effect takes place indicating that the rate constant decreases the number of carbon atoms (C_4, C_6, and C_8) on R group as initiator increases. Second, for the effect of branching initiators; $Sn(n\text{-OBut})_2$, $Sn(i\text{-OBut})_2$ and $Sn(t\text{-OBut})_2$, it is found that the more branch of side chains, the more steric effect increases resulting in decreasing of rate constants.

Conclusions

DFT calculations of stationary points along the reaction pathway in the ROP of CL initiated by tin(II) alkoxides give insight into the addition detailed mechanisms of their initiation and propagation processes. Transition states having four-membered rings are found in all cases and the apparent energy barriers of initiation (energy differences between **complex** and **TS1**) of CL with different $Sn(OR)_2$ initiators as R=*n*-But, *i*-But, *t*-But, *n*-Hex, *n*-Oct are calculated to be 14.58, 14.61, 14.59, 15.04, and 20.04 kcal mol^{-1}, respectively. The $Sn(OR)_2$ with R having *n*-But has the lowest apparent energy barriers resulting in the fastest rate constant under the same condition among all five initiators. The calculated rate constants of all initiators by transition state theory are in good agreement with experimental results. Such studies may be applicable to ROP of lactide initiated by tin(II) alkoxides and also ring-opening of cyclic ester by metal alkoxide initiators.

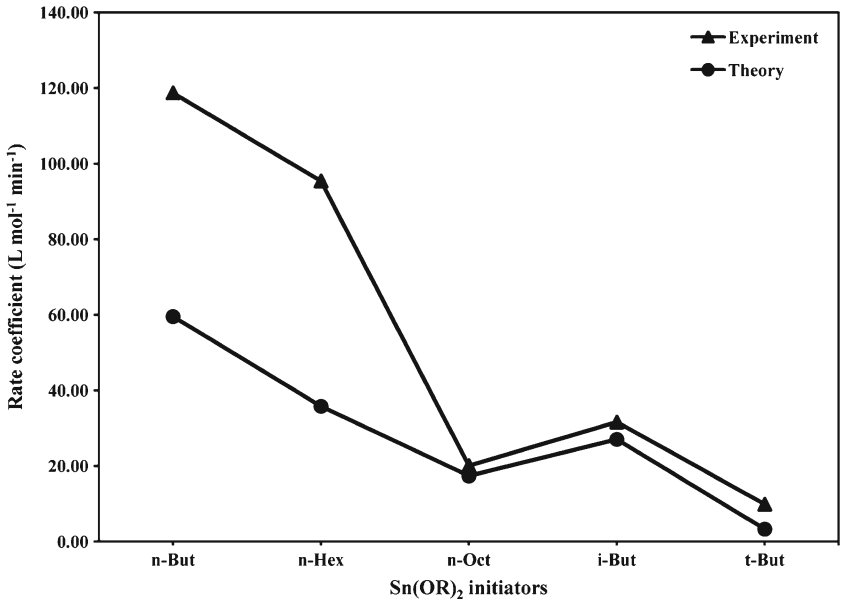

Fig. 4 The rate coefficient of all reactions in ROP of CL initiated by tin(II) alkoxide series, calculated at 120 °C

Acknowledgments The authors wish to thank the National Research University Project under Thailand's Office of the Higher Education Commission for financial support and National Science and Technology Development Agency (NSTDA). C. Sattayanon gratefully thanks the Center for Innovation in Chemistry (PERCH-CIC), Department of Chemistry, Faculty of Science, Chiang Mai University. And the Graduate School of Chiang Mai University is also acknowledged.

References

1. Gross RA, Kalra B (2002) Biodegradable polymers for the environment. Science (Washington, DC, U S) 297:803–807. doi:10.1126/science.297.5582.803
2. Chang RK, Price J, Whitworth CW (1987) Control of drug release rate by use of mixtures of polycaprolactone and cellulose acetate butyrate polymers. Drug Dev Ind Pharm 13(6):1119–1135
3. Chang RK, Price JC, Whitworth CW (1986) Control of drug release rates through the use of mixtures of polycaprolactone and cellulose propionate polymers. Pharm Technol 10(10):24, 26, 29, 32–23
4. Chasin M, Langer R eds (1990) Drugs and the pharmaceutical sciences, vol. 45. Biodegradable polymers as drug delivery systems. Dekker, New York
5. Edlund U, Albertsson AC (2002) Degradable polymer microspheres for controlled drug delivery. In: Degradable aliphatic polyesters, vol 157. Advances in polymer science. Springer, Berlin, pp 67–112
6. Perrin DE, English JP (1997) Polycaprolactone. Drug Target Deliv 7:63–77. In: Handbook of biodegradable polymers. Harwood, Amsterdam
7. Kumar D (2011) Biodegradable polymers and packaging: go green. Pop Plast Packag 56:24–32 Reserved
8. Jérôme C, Lecomte P (2008) Recent advances in the synthesis of aliphatic polyesters by ring-opening polymerization. Adv Drug Deliv Rev 60(9):1056–1076
9. Albertsson A-C, Varma IK (2003) Recent developments in ring opening polymerization of lactones for biomedical applications. Biomacromolecules 4(6):1466–1486. doi:10.1021/bm034247a
10. Kamber NE, Jeong W, Waymouth RM, Pratt RC, Lohmeijer BGG, Hedrick JL (2007) Organocatalytic ring-opening polymerization. Chem Rev (Washington, DC, U S) 107:5813–5840. doi:10.1021/cr068415b
11. von Schenck H, Ryner M, Albertsson A-C, Svensson M (2002) Ring-opening polymerization of lactones and lactides with Sn(IV) and Al(III) initiators. Macromolecules 35(5):1556–1562. doi:10.1021/ma011653i
12. Gadzinowski M, Sosnowski S, Slomkowski S (1996) Kinetics of the dispersion ring-opening polymerization of ε-caprolactone initiated with diethylaluminum ethoxide. Macromolecules 29(20):6404–6407. doi:10.1021/ma9600466
13. Chen H-Y, Huang B-H, Lin C-C (2005) A Highly efficient initiator for the ring-opening polymerization of lactides and ε-caprolactone: a kinetic study. Macromolecules 38(13):5400–5405. doi:10.1021/ma050672f
14. Li P, Zerroukhi A, Chen J, Chalamet Y, Jeanmaire T, Xia Z (2009) Synthesis of poly([var epsilon]-caprolactone)-block-poly(n-butyl acrylate) by combining ring-opening polymerization and atom transfer radical polymerization with Ti[OCH2CCl3]4 as difunctional initiator: I. Kinetic study of Ti[OCH2CCl3]4 initiated ring-opening polymerization of [var epsilon]-caprolactone. Polymer 50(5):1109–1117
15. Meelua W, Bua-own V, Molloy R, Punyodom W (2012) Comparison of metal alkoxide initiators in the ring-opening polymerization of caprolactone. Adv Mater Res (Durnten-Zurich, Switz) 506:142–145. doi:10.4028/www.scientific.net/AMR.506.142
16. Meelua W, Molloy R, Meepowpan P, Punyodom W (2012) Isoconversional kinetic analysis of ring-opening polymerization of ε-caprolactone: steric influence of titanium(IV) alkoxides as initiators. J Polym Res 19:1–11. doi:10.1007/s10965-011-9799-8
17. Li X, Zhu Y, Ling J, Shen Z (2012) Direct cyclodextrin-mediated ring opening polymerization of ε-caprolactone in the presence of yttrium trisphenolate catalyst. Macromol Rapid Commun 33:1008–1013. doi:10.1002/marc.201100848
18. Ling J, Liu J, Shen Z, Hogen-Esch TE (2011) Ring-opening polymerization of .vepsiln.-caprolactone catalyzed by Yttrium trisphenolate in the presence of 1,2-propanediol: Do both primary and secondary hydroxyl groups initiate polymerization? J Polym Sci, Part A Polym Chem 49:2081–2089. doi:10.1002/pola.24637
19. Kowalski A, Duda A, Penczek S (2000) Mechanism of cyclic ester polymerization initiated with tin(II) octoate. 2. Macromolecules fitted with tin(II) alkoxide species observed directly in MALDI-TOF spectra. Macromolecules 33(3):689–695
20. Kricheldorf HR, Bornhorst K, Hachmann-Thiessen H (2005) Bismuth(III) n-hexanoate and tin(II) 2-ethylhexanoate initiated copolymerizations of ε-caprolactone and l-lactide. Macromolecules 38(12):5017–5024. doi:10.1021/ma047873o
21. Kowalski A, Libiszowski J, Biela T, Cypryk M, Duda A, Penczek S (2005) Kinetics and mechanism of cyclic esters polymerization initiated with tin(II) octoate. polymerization of ε-caprolactone and l, l-lactide co-initiated with primary amines. Macromolecules 38(20):8170–8176. doi:10.1021/ma050752j
22. Sobczak M, Kolodziejski W (2009) Polymerization of cyclic esters initiated by carnitine and tin (II) octoate. Molecules 14(2):621–632
23. Sobczak M (2012) Ring-opening polymerization of cyclic esters in the presence of choline/SnOct2 catalytic system. Polym Bull 68(9):2219–2228. doi:10.1007/s00289-011-0676-8
24. Fernández J, Meaurio E, Chaos A, Etxeberria A, Alonso-Varona A, Sarasua JR (2013) Synthesis and characterization of poly (l-lactide/ε-caprolactone) statistical copolymers with well resolved chain microstructures. Polymer 54(11):2621–2631. doi:10.1016/j.polymer.2013.03.009
25. Dumklang M, Pattawong N, Punyodom W, Meepowpan P, Molloy R, Hoffman M (2009) Novel tin(II) butoxides for use as initiators in the ring-opening polymerisation of ε-caprolactone. Chiang Mai J Sci 36:136–148
26. Kleawkla A, Molloy R, Naksata W, Punyodom W (2008) Ring-opening polymerization of ε-caprolactone using novel tin(II) alkoxide initiators. Adv Mater Res (Zuerich, Switz) 55–57:757–760. doi:10.4028/www.scientific.net/AMR.55-57.757
27. Jerome R, Lecomte P (2005) New developments in the synthesis of aliphatic polyesters by ring-opening polymerisation. Woodhead, Cambridge, pp 77–106. doi:10.1533/9781845690762.1.77
28. Albertsson A-C, Varma IK (2002) Aliphatic polyesters: synthesis, properties and applications. Adv Polym Sci 157:1–40
29. Liu J, Ling J, Li X, Shen Z (2009) Monomer insertion mechanism of ring-opening polymerization of [var epsilon]-caprolactone with yttrium alkoxide intermediate: a DFT study. J Mol Catal A Chem 300(1–2):59–64
30. Ling J, Shen J, Hogen-Esch TE (2009) A density functional theory study of the mechanisms of scandium-alkoxide initiated coordination-insertion ring-opening polymerization of cyclic esters. Polymer 50:3575–3581. doi:10.1016/j.polymer.2009.06.006
31. Ni X, Liang Z, Ling J, Li X, Shen Z (2011) Controlled ring-opening polymerization of ε-caprolactone initiated by in situ formed yttrium trisalicylaldimine complexes, and their study by density functional theory. Polym Int 60:1745–1752. doi:10.1002/pi.3145
32. Delcroix D, Couffin A, Susperregui N, Navarro C, Maron L, Martin-Vaca B, Bourissou D (2011) Polym Chem 2:2249–2256. doi:10.1039/c1py00210d
33. Susperregui N, Kramer MU, Okuda J, Maron L (2011) Theoretical study on the ring-opening polymerization of ε-caprolactone by [YMeX(THF)5]+ with X = BH4, NMe2. Organometallics 30:1326–1333. doi:10.1021/om100606p

34. Stephens PJ, Devlin FJ, Chabalowski CF, Frisch MJ (1994) Ab initio calculation of vibrational absorption and circular dichroism spectra using density functional force fields. J Phys Chem 98(45):11623–11627. doi:10.1021/j100096a001
35. Hay PJ, Wadt WR (1985) Ab initio effective core potentials for molecular calculations. Potentials for the transition metal atoms Sc to Hg. J Chem Phys 82(1):270–283
36. Wadt WR, Hay PJ (1985) Ab initio effective core potentials for molecular calculations. Potentials for main group elements Na to Bi. J Chem Phys 82(1):284–298
37. Ryner M, Stridsberg K, Albertsson A-C, von Schenck H, Svensson M (2001) Mechanism of ring-opening polymerization of 1,5-dioxepan-2-one and l-lactide with stannous 2-ethylhexanoate. A theoretical study. Macromolecules 34(12):3877–3881. doi:10.1021/ma002096n
38. Eguiburu JL, Fernandez-Berridi MJ, Cossio FP, Roman JS (1999) Ring-opening polymerization of l-lactide initiated by (2-methacryloxy)ethyloxy-aluminum trialkoxides. 1. kinetics. Macromolecules 32(25):8252–8258. doi:10.1021/ma990445b
39. Hratchian HP, Schlegel HB (2004) Accurate reaction paths using a Hessian based predictor-corrector integrator. J Chem Phys 120:9918–9924. doi:10.1063/1.1724823
40. Zhu R, Wang R, Zhang D, Liu C (2009) A density functional theory study on the ring-opening polymerization of d-lactide catalyzed by a bifunctional-thiourea catalyst. Aust J Chem 62(2):157–164. doi:10.1071/CH08118
41. Frisch GWT MJ, Schlegel HB, Scuseria GE, Robb MA, Cheeseman JR, Montgomery JA Jr, Vreven T, Kudin KN, Burant JC, Millam JM, Iyengar SS, Tomasi J, Barone V, Mennucci B, Cossi M, Scalmani G, Rega N, Petersson GA, Nakatsuji H, Hada M, Ehara M, Toyota K, Fukuda R, Hasegawa J, Ishida M, Nakajima T, Honda Y, Kitao O, Nakai H, Klene M, Li X, Knox JE, Hratchian HP, Cross JB, Bakken V, Adamo C, Jaramillo J, Gomperts R, Stratmann RE, Yazyev O, Austin AJ, Cammi R, Pomelli C, Ochterski JW, Ayala PY, Morokuma K, Voth GA, Salvador P, Dannenberg JJ, Zakrzewski VG, Dapprich S, Daniels AD, Strain MC, Farkas O, Malick DK, Rabuck AD, Raghavachari K, Foresman JB, Ortiz JV, Cui Q, Baboul AG, Clifford S, Cioslowski J, Stefanov BB, Liu G, Liashenko A, Piskorz P, Komaromi I, Martin RL, Fox DJ, Keith T, Al-Laham MA, Peng CY, Nanayakkara A, Challacombe M, Gill PMW, Johnson B, Chen W, Wong MW, Gonzalez C, Pople JA (2004) Gaussian 03 (Revision E.01). Gaussian, Inc, Wallingford
42. Khanna A, Sudha Y, Pillai S, Rath S (2008) Molecular modeling studies of poly lactic acid initiation mechanisms. J Mol Model 14(5):367–374
43. Truong TN, Zhang S (2001) VKLab version 1.0. University of Utah, Salt Lake